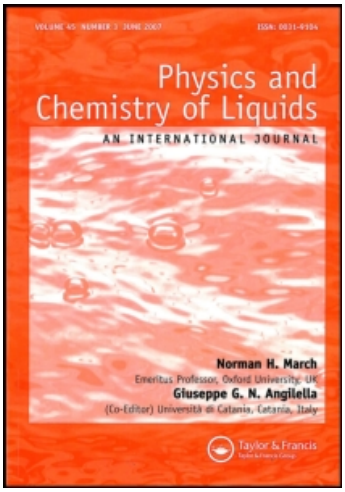

Physics and Chemistry of Liquids
Publication details, including instructions for authors and subscription information:
http://www.informaworld.com/smpp/title~content=t713646857

The structure factor for liquid lead

U. Dahlborg[a]; M. Davidovic[ab]; K. E. Larsson[a]
[a] Department of Reactorphysics, Royal Institute of Technology, Stockholm, Sweden [b] "Boris Kidric" Institute, Belgrade, Yugoslavia

To cite this Article Dahlborg, U. , Davidovic, M. and Larsson, K. E.(1977) 'The structure factor for liquid lead', Physics and Chemistry of Liquids, 6: 3, 149 — 166
To link to this Article: DOI: 10.1080/00319107708084137
URL: http://dx.doi.org/10.1080/00319107708084137

Phys. Chem. Liq., 1977, Vol. 6, pp. 149–166

Printed in Great Britain

The Structure Factor for Liquid Lead

U. DAHLBORG, M. DAVIDOVIC,† and K. E. LARSSON

Department of Reactorphysics, Royal Institute of Technology, Stockholm, Sweden.

(*Received April 18, 1977*)

The structure factor for liquid lead at the temperatures 613 K, 643 K, 863 K and 1163 K are measured by neutron diffraction. Extensive comparisons to earlier measurements are made as well as comparisons to different hard-core models.

INTRODUCTION

In recent years there has been a renewed interest in the determination of the static structure factor for liquids.[1,2] A detailed knowledge of this quantity is essential in order to obtain an effective inter-particle potential. Several different schemes, all approximate to some degree, exist in order to extract the potential from the measured data. The most common way has been to use the so-called hypernetted-chain equation (HNC) and the Percus–Yevick equation (PY).[3] The results are, however, discouraging as the obtained pair potentials are rather different from the ones obtained from pseudopotential theory.

However, lately new more successful approaches have appeared. The "thermodynamic consistency" scheme proposed by Brennan *et al.*,[4] has given an improved pair-potential for neon. Of great interest is the theory by Weeks, Chandler and Anderson.[1,5] Recently Mitra and Gillan[6] noticed the possibility of inverting the WCA theory. These new approaches have clearly demonstrated that in dense monoatomic liquids the structure of the liquid is dominated by the repulsive part of the interatomic potential and that the slowly varying attractive part can be treated as a perturbation.

In this paper the neutron diffraction technique is used to obtain the liquid Pb structure factor at four different temperatures. Extensive comparisons

† On leave of absence from the "Boris Kidric" Institute, Vinca, Belgrade, Yugoslavia. Now returned.

to earlier measurements are made as well as comparisons to different hard-core models.

GENERAL THEORY

The liquid structure factor ($S(Q)$) which is related to the measured intensities in neutron and X-ray diffraction experiments is defined in an isotropic fluid as

$$S(Q) = 1 + 4\pi n \int_0^\infty R^2[g(R) - 1]j_0(QR)\mathrm{d}R \tag{1}$$

where hQ is the momentum transfer in the scattering process. $g(R)$ is the pair distribution function and n the number density. Thus the number of atoms in a shell of thickness $\mathrm{d}R$ at distance R from an atom at the origin is given by $4\pi nR^2g(R)\mathrm{d}R$.

From Eq. (1) it is seen that, in principle, from a measurement of $S(Q)$ the pair distribution function $g(R)$ is obtained via a Fourier transform. However, as will be discussed below many corrections have to be imposed on the measured intensity in order to achieve $S(Q)$. Also the restricted range of Q values which are experimentally obtainable gives rise to some ambiguity in the Fourier transformation procedure.

In order to proceed further and obtain a formal relation between $S(Q)$ and the inter-particle pair potential the direct correlation function $c(R)$ is defined as

$$c(R) = (2\pi^2R)^{-1} \int_0^\infty Q\tilde{c}(Q)\sin QR\,\mathrm{d}Q \tag{2}$$

where

$$n\tilde{c}(Q) = 1 - \frac{1}{S(Q)}$$

The intermolecular potential $u(R)$ is related to $g(R)$ through a cluster expansion. However, to obtain relations suitable for numerical calculations several approximations have to be made. The two most commonly used direct methods are the HNC and the PY equations.[3] These can be written

$$u(R)_{\mathrm{PY}} = k_BT \ln\left[1 - \frac{c(R)}{g(R)}\right],$$

$$u(R)_{\mathrm{HNC}} = k_BT[g(R) - c(R) - 1 - \ln g(R)] \tag{3}$$

where k_B is the Boltzman constant and T the temperature in degrees K. The two equations are obtained from different truncations of higher order cluster diagrams. In spite of containing some diagrams less the PY equation mostly gives better results than the HNC equation. It is also possible to derive an exact solution for a fluid of hard spheres in the PY recipe. This will be discussed below.

EXPERIMENTAL DETAILS

The neutron-diffraction patterns were obtained using one of the crystal spectrometers at the Studsvik reactor. The wave length of the incident neutrons was 1.06 Å. Two different collimations were employed in order to ensure that no resolution broadening of the main diffraction peak was present. Most measurements were performed with a resolution of $\Delta Q \simeq 0.05$ Å^{-1}. The range of momentum transfer covered was 0.85 Å$^{-1} \leq Q \leq 9.7$ Å^{-1}.

The measurements were performed at 340 C, 370 C, 590 C and 890 C. The sample was in the shape of a slab of size 6×8 cm^2 and of thickness 3.2 mm. The temperature was controlled with an accuracy of ± 2 C. The sample container was made of a molybdenum frame with 0.5 mm thick windows. In order to keep the number of background Bragg peaks as small as possible molybdenum wires were used for heating and molybdenum sheets as radiation shields. The sample arrangement was placed in a water-cooled aluminium vacuum chamber.

TREATMENT OF DATA

The procedure for extraction of the structure factor, $S(Q)$, from measured angular distributions of scattered neutrons has been fully discussed by North *et al.*,[7] and here only a few points will be briefly mentioned.

In spite of the attempts to reduce the background several Bragg peaks from molybdenum were seen in the measured spectra. After subtraction of the background some small bumps remained at the positions of Mo(211) and Mo(310) Bragg peaks. To avoid irregularities in the spectra these bumps were removed by at least square procedure.

The contribution of multiple scattering from the sample was calculated from the computer program of Cocking and Heard[8] and found to amount to about 20% of the single scattering intensity. However, after normalization of the data to absolute cross section units via a vanadium calibration run it was noticed that the intensity at small Q-values was substantially higher

than expected from theoretical reasons. This additional intensity was most probably due to multiple scattering in the sample container and the furnace. The effect is possible to simulate with the multiple scattering program developed by Copley.[9] It was, however, concluded that a proper normalization of the measured structure factor could easier be achieved from the known values of $S(Q)$ for large and small Q. Both ways of normalization involves several difficulties but should yield the same result.

From the known properties of $S(Q)$ it is easily seen that

$$S(Q) = \alpha S(Q)_{\text{meas}} + \beta \tag{4}$$

where

$$\alpha = \frac{[1 - S(0)_{\text{theor}}]}{[S(\infty)_{\text{meas}} - S(0)_{\text{meas}}]}$$

$$\beta = \frac{[S(\infty)_{\text{meas}} \cdot S(0)_{\text{theor}} - S(0)_{\text{meas}}]}{[S(\infty)_{\text{meas}} - S(0)_{\text{meas}}]}$$

The two quantities $S(0)_{\text{meas}}$ and $S(\infty)_{\text{meas}}$ have to be extracted from the measured distributions.

The limiting value of the structure factor for large Q was obtained from a least squares fitting of

$$S(Q)_{\text{meas}} = C_1 + C_2 \cos[C_3 Q - C_4]\exp(-C_5 Q) \tag{5}$$

to the measured intensity distribution for $Q > 3.2\ \text{Å}^{-1}$. The agreement between the calculated and the measured values is good and thus the determination of $S(\infty)_{\text{meas}} = C_1$ seems to be unambiguous. Some parameter values from the fit at 613 K are given in Table I.

TABLE I

	Fit of $S(Q) = C_1 + C_2 \cos(C_3 Q - C_4)e^{-C_5 Q}$		Consistency checks	
T K	C_3	C_5	Eq. (8)	Eq. (9)
613	3.28	0.44	0.97	0.89
643	3.29	0.48	0.87	0.89
863	3.38	0.53	0.88	0.92
1163	3.14	0.56	0.97	0.95

The extrapolated intensity at $Q = 0$ is, however, difficult to get. Several different ways were tried. The main principle was to avoid relying upon any other experimental work and also to avoid the arbitrariness which is involved in the subjective hand-drawing of curves through the data points.

Instead the following properties of $S(Q)$ and $g(R)$ were used:

i) From the compressibility equation the value of the structure factor at $Q = 0$ is found to

$$S(0)_{\text{theor}} = \chi_T n k_B T \tag{6}$$

where χ_T is the isothermal compressibility.

ii) As was discussed above the pair distribution function is in principle obtainable from a measured $S(Q)$. Uncertainties of the extrapolations of $S(Q)$ to $Q = 0$ and to $Q \to \infty$ introduce, however, difficulties in the numerical computation. Another problem is the statistical nature of the measured intensities. The resulting $g(R)$ usually shows ripples at small R. As real molecules can not penetrate each other the value of $g(R)$ inside the hard core must be negligible. Thus in order to obtain $S(0)_{\text{meas}}$ an iterative computational scheme was adopted:

1) A value $S(0)_{\text{meas}} = a$ is chosen

2) $S(Q)$ between $Q = 0$ and the first measured point at $Q = 0.85$ Å^{-1} is assumed to be parabolic[10] and given by

$$S(Q) = a + [S(0.85) - a]\left(\frac{Q}{0.85}\right)^2 \tag{7}$$

3) $S(Q)$ is extrapolated and normalized according to Eq. (4).

4) $g(R)$ is obtained via Eq. (1).

A "best" value for $S(0)_{\text{meas}}$ was chosen so that the expressions

$$\int_0^{1.5} |g(R)| \mathrm{d}R \quad \text{and} \quad \int_0^{1.5} g(R) \mathrm{d}R$$

had their minimum values. It should be stressed that the ripples in $g(R)$ for small R does not disappear through this iteration process (compare Figure 6 below).

The resulting normalized structure factors at four temperatures (613 K, 643 K, 863 K and 1163 K) are shown in Figure 1 and listed in Table II. The total error in each point due to the contribution of statistical and normalization errors is about ± 0.02.

There are at least two consistency criteria $S(Q)$ and the distribution functions derived from $S(Q)$ must fulfill.[15] One is the sum rule which results from the fact that $g(R) = 0$ at $R = 0$.

$$(2\pi^2 n)^{-1} \int_0^{\infty} [1 - S(Q)] Q^2 \, \mathrm{d}Q = 1 \tag{8}$$

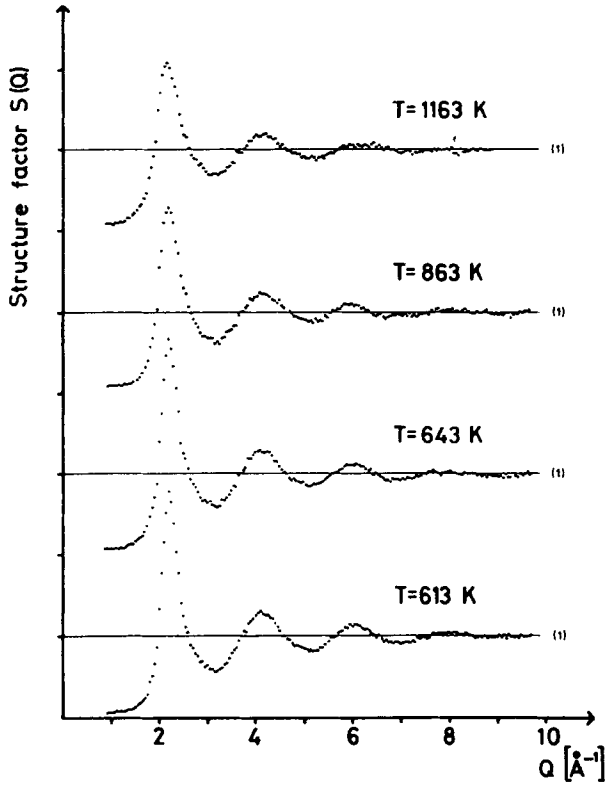

FIGURE 1 Normalized structure factors for liquid lead at four temperatures.

A second criterium follows directly from the compressibility equation

$$4\pi n\left(1 - \frac{1}{\chi_T n k_B T}\right)^{-1} \int_0^\infty c(R)R^2\,dR = 1 \tag{9}$$

It is obvious from a study of the integrands that Eq. (8) is most sensitive to the large Q region and thus yields a test of the accuracy of Eq. (5). On the other hand the largest contribution in Eq. (9) comes from the small Q region in $S(Q)$. The values of the left hand sides of Eqs. (8) and (9) are given in Table I. All values are low but satisfactorily close to one. It is possible to obtain the correct values by making "adjustments" of the data within the limits of error.[12,16] However, we do not feel that this is an allowed method and prefer to leave the data "unadjusted". As will be seen below the small Q part of $S(Q)$ is of particular significance in the calculation of the direct correlation function $c(R)$. Figure 2 shows this region on an enlarged scale. The neutron data taken from Enderby[3] are shown as filled circles while the X-ray data

Normalized structure factors for liquid lead.

Q(Å^{-1})	613 K	643 K	863 K	1163 K	Q(Å^{-1})	613 K	643 K	863 K	1163 K	Q(Å^{-1})	613 K	643 K	863 K	1163 K
0.9	0.072	0.070	0.082	0.080										
1.0	0.073	0.066	0.085	0.084	4.0	1.261	1.273	1.185	1.161	7.0	0.912	0.918	0.967	0.963
1.1	0.077	0.077	0.093	0.090	4.1	1.311	1.307	1.245	1.168	7.1	0.933	0.928	0.974	0.964
1.2	0.080	0.076	0.093	0.098	4.2	1.269	1.264	1.225	1.197	7.2	0.916	0.946	0.949	0.976
1.3	0.089	0.090	0.101	0.107	4.3	1.235	1.279	1.198	1.167	7.3	0.926	0.943	0.963	0.935
1.4	0.104	0.111	0.118	0.153	4.4	1.164	1.162	1.141	1.141	7.4	0.974	0.965	0.964	0.962
1.5	0.126	0.148	0.175	0.203	4.5	1.071	1.090	1.152	1.081	7.5	0.994	0.998	0.974	0.969
1.6	0.189	0.201	0.258	0.290	4.6	1.010	1.023	1.047	1.067	7.6	0.994	1.026	0.972	0.989
1.7	0.250	0.248	0.326	0.393	4.7	0.958	0.947	1.014	0.985	7.7	1.043	1.050	1.000	0.975
1.8	0.449	0.469	0.567	0.647	4.8	0.890	0.943	0.953	0.959	7.8	1.048	1.007	1.043	0.981
1.9	0.666	0.703	0.852	0.917	4.9	0.882	0.899	0.931	0.947	7.9	1.043	1.016	1.021	0.995
2.0	1.340	1.402	1.574	1.494	5.0	0.859	0.896	0.909	0.902	8.0	1.055	1.031	1.030	1.005
2.1	2.154	2.181	2.089	1.928	5.1	0.811	0.837	0.874	0.883	8.1	1.052	1.014	1.038	1.035
2.2	2.783	2.677	2.278	2.084	5.2	0.821	0.866	0.863	0.918	8.2	1.035	1.008	1.015	0.998
2.3	2.376	2.348	2.100	1.894	5.3	0.827	0.878	0.881	0.852	8.3	1.026	0.988	1.017	1.007
2.4	1.770	1.782	1.737	1.676	5.4	0.869	0.898	0.889	0.905	8.4	1.018	1.005	1.003	0.972
2.5	1.253	1.263	1.290	1.298	5.5	0.940	0.956	0.934	0.925	8.5	1.006	1.003	0.992	0.987
2.6	1.050	1.061	1.060	1.156	5.6	0.983	0.998	1.019	0.962	8.6	0.988	0.970	0.995	0.982
2.7	0.855	0.869	0.914	0.929	5.7	1.053	1.023	1.041	0.991	8.7	0.981	0.971	0.984	1.013
2.8	0.762	0.768	0.817	0.870	5.8	1.068	1.058	1.070	1.025	8.8	0.977	0.959	1.005	0.995
2.9	0.703	0.662	0.705	0.823	5.9	1.109	1.120	1.100	1.042	8.9	0.965	0.978	0.975	0.997
3.0	0.649	0.645	0.684	0.718	6.0	1.128	1.107	1.104	1.064	9.0	0.995	0.971	0.985	0.998
3.1	0.599	0.610	0.670	0.681	6.1	1.143	1.130	1.091	1.029	9.1	0.984	0.971	0.971	
3.2	0.580	0.580	0.625	0.695	6.2	1.104	1.094	1.044	1.057	9.2	0.969	0.995	0.984	
3.3	0.623	0.682	0.679	0.700	6.3	1.089	1.063	1.026	1.059	9.3	0.995	0.968	0.979	
3.4	0.686	0.706	0.758	0.727	6.4	1.042	1.057	0.994	1.035	9.4	1.002	0.984	0.983	
3.5	0.803	0.789	0.786	0.790	6.5	0.988	1.008	0.984	1.025	9.5	1.013	0.998	1.002	
3.6	0.869	0.846	0.839	0.824	6.6	0.972	0.967	0.978	1.011	9.6	1.005	1.005	1.012	
3.7	1.012	1.008	0.993	0.962	6.7	0.953	0.922	0.947	0.992	9.7	1.027	0.997	1.029	
3.8	1.057	1.086	1.052	1.017	6.8	0.929	0.900	0.942	0.969					
3.9	1.195	1.191	1.162	1.114	6.9	0.930	0.928	0.957	0.996					

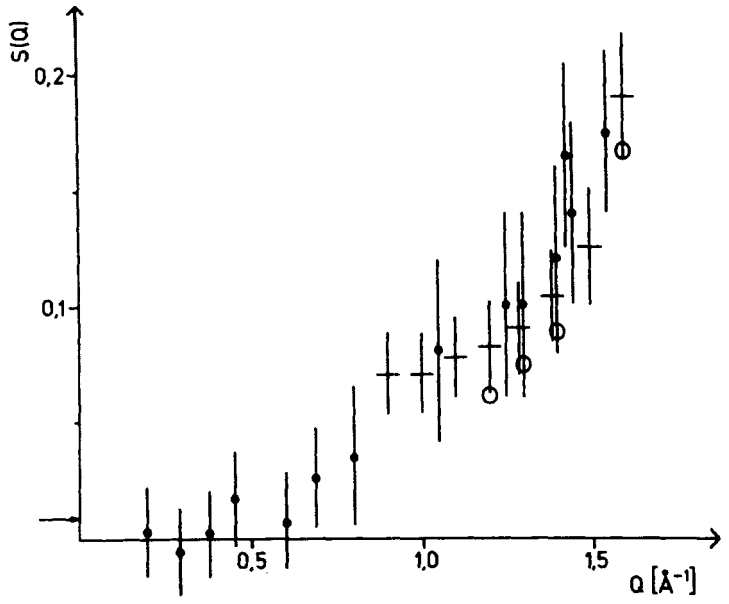

FIGURE 2 The structure factor at small momentum transfers. The filled circles are neutron data from Enderby, the open circles X-ray data from Steffen and the crosses are the present data. The arrow shows the thermodynamic limit of $S(Q)$.

from Steffen[14] are denoted by open circles. There is an agreement within limits of error between the different experiments. The small indication of a bump around $Q \simeq 1\,\text{Å}^{-1}$ might be fortuitous. In the near future accurate experiments to clarify this point will be performed.

The general effect on $S(Q)$ on heating is a general smearing out of its structure. In order to obtain a more quantitative idea about the effect the quantity $(T/S(Q)) \cdot (\Delta S(Q)/\Delta T)$ is plotted as vertical lines in Figure 3. Average over three combinations of $S(Q)$ has been taken. The average temperature is 793 K. The open circles are the X-ray data of Steffen.[14] The value for $Q = 0$ (cross) is calculated from the known temperature variation of the compressibility. Even if there is a difference around $Q = 2.1\,\text{Å}^{-1}$ between the X-ray and the neutron data they both indicate the existence of a minimum between $Q = 1.1\,\text{Å}^{-1}$ and $Q = 1.3\,\text{Å}^{-1}$. This has not been demonstrated earlier as known to the authors. The physical background for this minimum is not understood.

In Table III some pertinent quantities of measured structure factors by different experimentalists are collected. Surprisingly there is a large spread in the height of the main peak of $S(Q)$ among the different measurements.

TABLE III

Comparison of measured structure factors $S(Q)$.

Reference	T C	First maximum		First minimum		Second maximum		Third maximum	
		Q Å^{-1}	$S(Q)$	Q Å^{-1}	$S(Q)$	Q Å^{-1}	$S(Q)$	Q Å^{-1}	$S(Q)$
A	329	2.19	2.78	3.19	0.59	4.11	1.30	6.09	1.10
B	340	2.23	2.60	3.13	0.63	4.20	1.34	6.04	1.10
C	340	2.28	2.46	3.15	0.63	4.23	1.29	6.17	1.11
D	350	2.20	2.66	3.13	0.57	4.10	1.29	6.05	1.11
E	340	2.21	2.79	3.15	0.58	4.10	1.30	6.05	1.13
A	600	2.19	2.35	3.19	0.64	4.18	1.25	6.09	1.08
B	600	2.23	2.09	3.13	0.69	4.15	1.18	6.07	1.07
D	550	2.20	2.27	3.11	0.62	4.15	1.25	6.10	1.10
E	590	2.20	2.28	3.15	0.64	4.12	1.24	6.05	1.10

A: Kaplow *et al.*, (Ref. 11)
B: North *et al.*, (Ref. 12)
C: Waseda *et al.*, (Ref. 13)
D: Steffen *et al.*, (Ref. 14)
E: Present experiment.

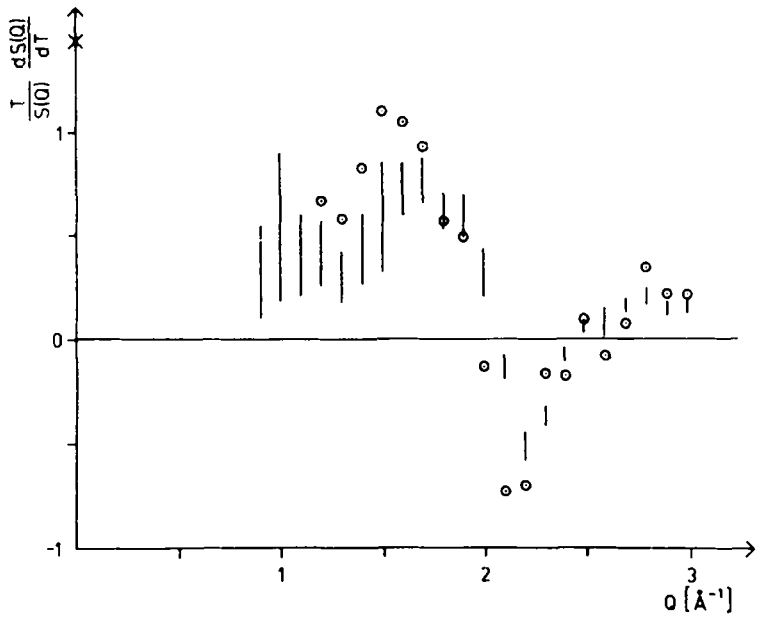

FIGURE 3 The temperature derivative of $S(Q)$. Open circles are X-ray data of Steffen and the vertical lines are the present data. The cross is calculated from the temperature variation of compressibility.

However, no significant trend with respect to X-ray diffraction results on one hand and neutron diffraction results on the other as suggested by Egelstaff *et al.*[17] can be seen.

COMPARISON TO HARD-CORE MODELS

Generally the repulsive intermolecular forces dominate the structure of a liquid and accordingly several thermodynamic properties can be explained by treating the ions as hard spheres. Therefore the attractive part of the potential can be introduced in this type of calculations via perturbation methods. Actually, the hard sphere fluid is treated as reference system and the attractive part as a perturbation to this reference system. Thus a direct comparison of the experimentally obtained structure factors to the predictions of different hard-core models is of considerable importance. Three models were chosen for this purpose:

i) The fundamental hard-core model is due to Ashcroft and Lekner[18] (AL) who used the solutions of the Percus–Yevick integral equations, re-

ported by Wertheim[19] and Thiele,[20] to obtain a closed expression for the structure factor. The result was

$$S(Q)_{AL} = [1 - n\tilde{c}(Q)]^{-1} \tag{10}$$

where

$$\begin{aligned} n\tilde{c}(Q) = & -24\eta(Q\sigma)^{-6}\{\alpha(Q\sigma)^3(\sin Q\sigma - Q\sigma\cos Q\sigma) \\ & + \beta(Q\sigma)^2[2Q\sigma\sin Q\sigma - (Q^2\sigma^2 - 2)\cos Q\sigma - 2] \\ & + \gamma[(4Q^3\sigma^3 - 24Q\sigma)\sin Q\sigma \\ & - (Q^4\sigma^4 - 12Q^2\sigma^2 + 24)\cos Q\sigma + 24]\} \end{aligned}$$

and

$$\begin{aligned} \alpha &= \frac{(1 + 2\eta)^2}{(1 - \eta)^4} \\ \beta &= \frac{-6\eta(1 + \eta/2)^2}{(1 - \eta)^4} \\ \gamma &= \frac{\eta\alpha}{2} \end{aligned} \tag{11}$$

The packing fraction η is related to the hard core diameter σ through $\eta = \pi n\sigma^3/6$.

ii) Using the more exact equation of state for hard spheres developed by Carnahan and Starling[21] the AL results were recently modified by Ailawadi[22] and by Sharma and Sharma (SS).[23] The only modification was in the parameters α and β which in the SS model take the form

$$\begin{aligned} \alpha &= \frac{[(1 + 2\eta)^2 + \eta^4 - 4\eta^3]}{(1 - \eta)^4} \\ \beta &= \frac{-\eta}{3}\,\frac{(18 + 20\eta - 12\eta^3 + \eta^4)}{(1 - \eta)^4} \end{aligned} \tag{12}$$

iii) The so called mean spherical model (MSM)[2] can be considered as a perturbation version of the AL model. The MSM assumes that the Percus-Yevick approximation is valid inside a hard core diameter while outside this distance an attractive potential is included by writing the direct correlation function as

$$c(R) = \frac{-u(R)}{k_B T} \quad (R > \sigma) \tag{13}$$

One advantage of the MSA approximation is that it can be solved analytically for several different potentials $u(R)$. We have chosen the square-well potential with depth ε and width λ.[24]

By a least squares procedure the three hard-core models were fitted to the measured structure factors over two different Q-regions, $1.8\,\text{Å}^{-1} \leq Q \leq 3.1\,\text{Å}^{-1}$ and $1.8\,\text{Å}^{-1} \leq Q \leq 6.0\,\text{Å}^{-1}$. The parameter values obtained from the two regions were almost exactly the same so only one set is given in Table IV.

TABLE IV

Derived values from fits of hard core models.

		AL model	SS model	MSM model		
T K	n atoms/Å^3	σ Å	σ Å	σ Å	ε meV	λ
613	0.03099	3.080	3.204	3.080	7.2	1.66
643	0.03088	3.070	3.180	3.070	7.3	1.66
863	0.03006	3.031	3.093	3.020	8.8	1.68
1163	0.02890	3.005	3.062	2.990	4.6	1.62

It is seen in Figure 4 that there is a remarkably good agreement between measured and calculated structure factors. The main peak is somewhat better reproduced by the MSM model while for larger Q values the simple AL model seems to be better. As has been noticed earlier the curves are for large Q slightly out of phase with respect to the measured points. The SS model yields a packing fraction at the melting point 0.534 which is too high ($\eta \gtrsim 0.5$ is not permitted on physical grounds) and thus the SS model is not applicable to liquid lead. A similar behaviour has been seen in liquid titanium.[24]

As expected, however, it is obvious that the main features of a liquid structure factor is due to the repulsive part of the potential. It is also obvious that in order to obtain a realistic pair potential, i.e. a potential with a soft core and an attractive part, from a structure factor measurement the experimental data must be of very good quality.

Silbert *et al.*,[25] recently explored the correlation between measured structure factors and the entropy for liquid metals. The quantity which can be mostly easily compared from the two types of measurements is the packing fraction. In Figure 5 packing fractions derived from thermodynamic data are compared to the results from diffraction experiments. All data are reproduced from Figure 4 of the paper by Silbert *et al.*, except those from Steffen and the present ones which are obtained from AL model fits. The agreement between entropy data and diffraction data can not be stated as conclusive.

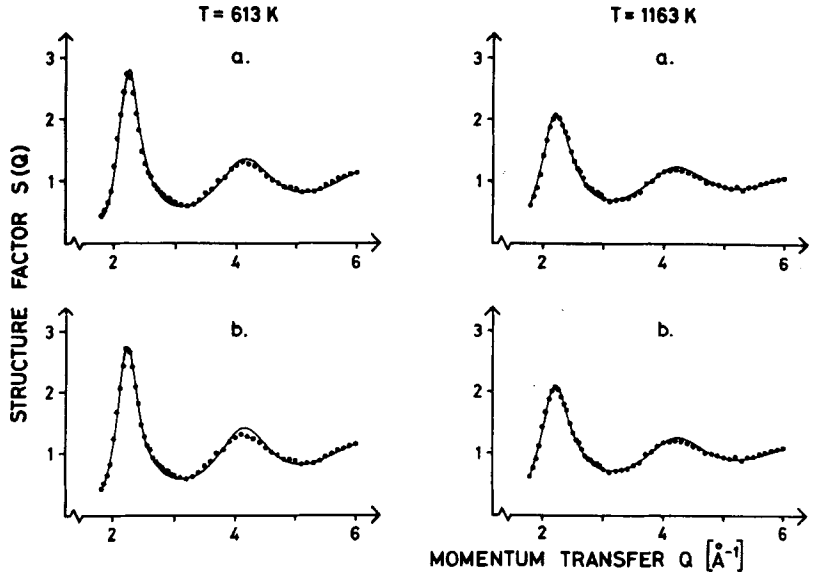

FIGURE 4 Calculated structure factors from AL (a) and MSM (b) models at 613 K and 1163 K. The circles are experimental points.

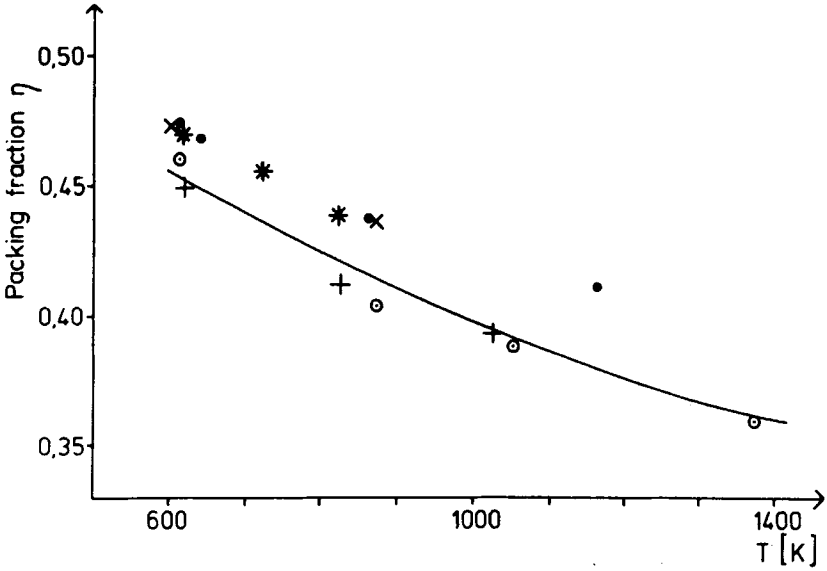

FIGURE 5 Experimentally obtained packing fractions compared to calculated ones (from Silbert *et al.*).

× X-ray data (ref. 11)
○ Neutron data (ref. 12)
\+ X-ray data (ref. 13)
* X-ray data (ref. 14)
● Neutron data (present)

THE PAIR DISTRIBUTION FUNCTION

The pair distribution functions $g(R)$, obtained from $S(Q)$ via a Fourier transform (Eq. 1), are shown in Figure 6. It is seen that spurious ripples occur at small R. This is an effect which definitely depends on how well $S(Q)$ satisfies the sum rule given in Eq. (8) (see Table I). There are many suggestions in the literature to "refine" the data thereby obtaining a ripple-free $g(R)$.[16] However, we do not feel convinced that experimental results should be "refined" and that if a refinement is made the result is unique. The amplitude of the ripples should instead be considered as a measure of the accuracy of the data normalization and of the termination errors in the Fourier transformation.

Some pertinent data for $g(R)$ at two temperatures are compared to results from other experiments in Table V. The agreement between the different

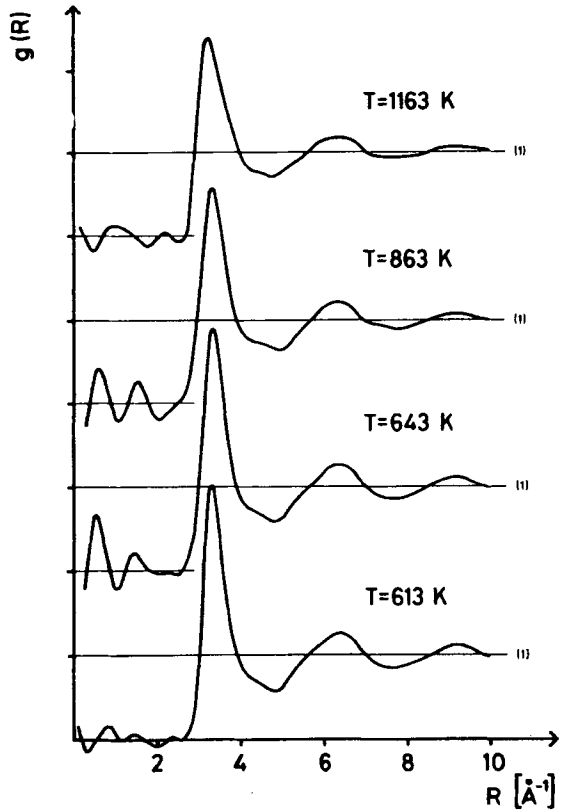

FIGURE 6 Derived pair distribution functions $g(R)$.

TABLE V

Comparison of derived pair distribution functions $g(R)$.

		First maximum		First minimum		Second maximum		Third maximum	
Reference	T C	R Å	$g(R)$	R Å	$g(R)$	R Å	$g(R)$	R Å	$g(R)$
A	329	3.42	2.77	4.80	0.63	6.52	1.27	9.25	1.11
B	340	3.34	2.80	4.61	0.63	6.35	1.27	9.17	1.10
C	340	3.23	2.09	4.52	0.64	6.18	1.28	9.12	1.08
D	350	3.40	2.77	4.77	0.63	6.49	1.25	9.33	1.10
E	340	3.34	3.00	4.85	0.59	6.45	1.27	9.25	1.11
A	600	3.30	2.67	4.90	0.70	6.43	1.22	9.35	1.07
B	600	3.28	2.46	4.87	0.71	6.42	1.22	9.17	1.06
D	550	3.33	2.49	4.74	0.71	6.43	1.19	9.30	1.06
E	590	3.36	2.58	4.93	0.65	6.48	1.22	9.25	1.07

A: Kaplow *et al.*, (Ref. 11)
B: North *et al.*, (Ref. 12)
C: Waseda *et al.*, (Ref. 13)
D: Steffen *et al.*, (Ref. 14)
E: Present experiment.

values except for those from Waseda *et al.*,[13] can be considered satisfactory. However, we do not feel the obtained $g(R)$ accurate enough in order to fit an analytical formula as suggested by Brostow.[26]

It has been quite customary to derive coordination numbers Z from measured $g(R)$. The problem of evaluating Z from $g(R)$ has been dealt with in detail by Pings.[10] Different methods can be used, all of them containing some degree of ambiguity. We have chosen to define Z from

$$Z = \int_0^{R_m} 4\pi R^2 n g(R) \mathrm{d}R \tag{17}$$

where R_m has been put equal to 4.45 Å. The obtained Z are 11.7, 11.7, 11.3 and 10.9 for the four measured temperatures (613 K, 643 K, 863 K and 1163 K).

THE DIRECT CORRELATION FUNCTION AND APPROXIMATE PAIR POTENTIALS

Direct correlation functions $c(R)$ derived from the experimental $S(Q)$ via Eq. (4) at two temperatures are shown in Figure 7a. The compressibility equation

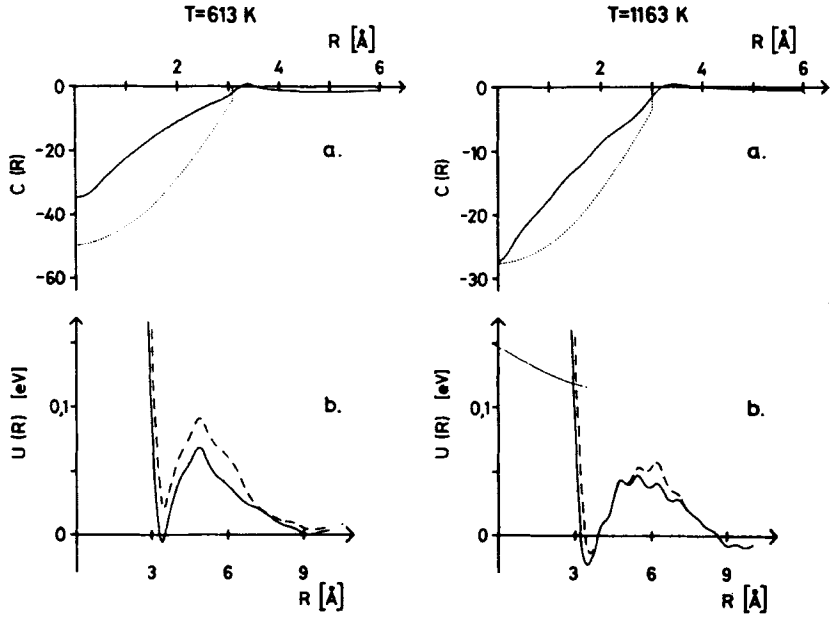

FIGURE 7 Derived direct correlation functions (a) and pair potentials (b). In (a) the full curve is obtained from the experimental data. The dotted one corresponds to the best fit of the AL model to the experimental $S(Q)$. In (b) the full curve is obtained via the PY equation and the broken one via the HNC equation.

is satisfied within about 10% which is considered to be satisfactory as $c(R)$ is a Fourier transform of the measured quantity. It was demonstrated in Figure 4 the experimental $S(Q)$ was to a high degree reproduced by a hard-sphere model in the sense that the difference between the measured and the fitted functions is small. However, the hard-sphere models do not yield the correct value for $S(0)$. For example, from the best fit at 613 K the hard-sphere model gave $S(0) = 0.020$ while the theoretical value calculated from Eq. (6) is 0.009. This difference which is indeed small on a absolute scale implies, however, that the corresponding direct correlation functions shown as dotted lines in Figure 7a are very different from the experimentally determined ones. As $c(R)$ is directly related to the pair potential this fact once again accentuates the need for an accurate measurement of $S(Q)$ in the small Q-region.

As was mentioned above there exists different methods to extract a pair potential from a structure factor. However, the methods have mostly failed to yield potentials of the shape which should be expected on physical grounds. Nevertheless, for the sake of completeness, we have calculated $u_{PY}(R)$ and $u_{HNC}(R)$ from our data by use of Eq. (3) for two different temperatures. The results are shown in Figure 7b and are similar to those of North *et al.*[12]

Acknowledgement

The authors wish to thank Dr. R. Stedman for putting a crystal spectrometer at our disposal and M. Grönros and L. E. Karlsson for skilful technical assistance.

References

1. H. C. Andersson, D. Chandler, and J. D. Weeks, Advances in Chemical Physics, Vol. 34, I. Prigogine and S. A. Rice (editors) Wiley, New York, 1976.
2. J. A. Barker and D. Henderson, *Rev. Mod. Phys.*, **48**, 587 (1976).
3. J. E. Enderby, Advances in Structure Research by Diffraction Methods, Vol. 4, W. Hoppe and R. Mason (editors), Pergamon Press, 1972.
4. M. Brennan, P. Hutchinson, M. J. L. Sangster, and P. Schofield, *J. Phys. C.*, **7**, L411 (1974).
5. R. Kumaravadivel and R. Evans, *J. Phys. C.*, **9**, 3877 (1976).
6. S. K. Mitra and M. J. Gillan, *J. Phys. C.*, **9**, L515 (1976).
7. D. M. North, J. E. Enderby, and P. A. Egelstaff, *J. Phys. C.*, **1**, 784 (1968).
8. S. J. Cocking and C. R. T. Heard, AERE-R5016 (1965).
9. J. R. D. Copley, *Comp. Phys. Comm.*, **7**, 289 (1974).
10. C. J. Pings, Physics in Simple Liquids, H. N. V. Temperly, J. S. Rowlinson, and G. S. Rushbroke (editors), North-Holland, 1968.
11. R. Kaplow, S. L. Strong, and B. L. Averbach, *Phys. Rev.*, **138**, A1336 (1965).
12. D. M. North, J. E. Enderby, and P. A. Egelstaff, *J. Phys. C.*, **1**, 1075 (1968).
13. Y. Waseda, K. Yokoyama, and K. Suzuki, *Phys. Chem. Liq.*, **4**, 267 (1975).
14. B. Steffen, *Phys. Rev.*, **B13**, 3227 (1976).
15. T. E. Faber, An Introduction to the Theory of Liquid Metals, Cambridge University Press, 1972.
16. K. R. Rao and B. A. Dasannacharya, *Pramana*, **5**, 328 (1975).
17. P. A. Egelstaff, N. H. March, and N. C. McGill, *Can. J. Phys.*, **52**, 1651 (1974).

18. N. W. Ashcroft and J. Lekner, *Phys. Rev.*, **145**, 83 (1966).
19. M. S. Wertheim, *Phys. Rev. L.*, **10**, 321 (1963).
20. E. Thiele, *J. Chem. Phys.*, **39**, 474 (1963).
21. N. F. Carnahan and K. E. Starling, *J. Chem. Phys.*, **51**, 635 (1969).
22. N. K. Ailawadi, *Phys. Rev.*, **A7**, 2200 (1973).
23. R. V. Sharma and K. C. Sharma, *Phys. L.*, **56A**, 107 (1976).
24. R. V. Gopala Rao and A. K. K. Murthy, *Phys. Stat. Sol.*, **66**, 703 (1974).
25. J. R. Todd and J. S. Brown, *Phys. L.*, **59A**, 302 (1976).
26. M. Silbert, I. H. Umar, M. Watabe, and W. H. Young, *J. Phys.*, **F5**, 1262 (1975).
27. W. Brostow and J. S. Sochanski, *Phys. Rev.*, **A13**, 882 (1976).